SCIENCE CHINA
Life Sciences

• RESEARCH PAPER •

June 2012 Vol.55 No.6: 533–541
doi: 10.1007/s11427-012-4316-9

Protein photo-folding and quantum folding theory

LUO LiaoFu

Faculty of Physical Science and Technology, Inner Mongolia University, Hohhot 010021, China

Received December 12, 2011; accepted March 28, 2012

The rates of protein folding with photon absorption or emission and the cross section of photon -protein inelastic scattering are calculated from quantum folding theory by use of a field-theoretical method. All protein photo-folding processes are compared with common protein folding without the interaction of photons (non-radiative folding). It is demonstrated that there exists a common factor (thermo-averaged overlap integral of the vibration wave function, TAOI) for protein folding and protein photo-folding. Based on this finding it is predicted that (i) the stimulated photo-folding rates and the photon-protein resonance Raman scattering sections show the same temperature dependence as protein folding; (ii) the spectral line of the electronic transition is broadened to a band that includes an abundant vibration spectrum without and with conformational transitions, and the width of each vibration spectral line is largely reduced. The particular form of the folding rate—temperature relation and the abundant spectral structure imply the existence of quantum tunneling between protein conformations in folding and photo-folding that demonstrates the quantum nature of the motion of the conformational-electronic system.

protein folding dynamics, photo-folding, conformational change, quantum transition

Citation: Luo L F. Protein photo-folding and quantum folding theory. Sci China Life Sci, 2012, 55: 533–541, doi: 10.1007/s11427-012-4316-9

Proteins are huge microscopic systems composed of several thousands of atoms. In principle, proteins should obey quantum laws. Recently, we proposed a protein quantum folding theory [1–3]. Although bioinformatics studies, such as the prediction of protein structure and function from molecular sequences, have achieved significant successes, the dynamic problem associated with protein folding remains unresolved. The proposed quantum folding theory emphasizes the concept of torsional cooperative transitions. The importance of a torsion state can be examined as the following: a multi-atom system, the conformation of a protein is fully determined by bond lengths, bond angles and torsion angles (dihedral angles). Torsion angles are the most easily changed of these three physical features, even at room temperature, and are usually assumed to be the main variables of a protein conformation. Simultaneously, the torsion potential generally has several minima, with the transition between minima responsible for conformational changes. All torsion modes between contact residues are taken into account in the proposed quantum folding theory. These modes are assumed to participate in the quantum transition cooperatively. In fact, the Bose condensation of strongly excited longitudinal electric modes represents an example of cooperativeness in living systems and was proposed in the 1970s [4,5]. The fold cooperativeness of a protein was also demonstrated in earlier literature [6]. These publications explained the possible existence of the cooperativeness in protein folding or in living systems from the point of non-linear dynamics and thermodynamics. More recently, contact order has been introduced as an important parameter for understanding and calculating the folding rate [7]. Meanwhile, the dihedral transition was observed more directly in the statistical analysis of protein conformational changes [8]. The cooperative dihedral transitions were found to occur in most (~82%) polypeptide chains. Based on the above considerations we formulated a quantum the-

email: lolfcm@mail.imu.edu.cn

© The Author(s) 2012. This article is published with open access at Springerlink.com

ory on non-radiative protein folding. The point of folding as a quantum transition can solve the folding speed problem (Levinthal's paradox)–how proteins can fold so fast when they can sample so many possible configurations [9]. In particular, the proposed theory can successfully interpret the non-Arrhenius behavior of the temperature dependence of folding rates [3].

To explore the fundamental physics behind the folding more deeply and to clarify the quantum nature of the folding mechanism more clearly we shall study the protein photo-folding processes, namely, the photon emission or absorption in protein folding and the inelastic scattering of photons on proteins (photon-protein resonance Raman scattering). Although fluorescent proteins have been extensively used as biological markers to observe gene and protein expression [10] and the fluorescence technique has been developed to examine protein folding and protein-protein interaction dynamics [11], quantitative theory on fluorescent transitions and its relation to protein folding remains unclear. The reason for this absence of information may be the complexity of the fluorescence mechanism, for example, many active proteins need a cofactor or other small molecules to fluoresce. An additional reason may be attributed to the prevalent "too-classical" understanding of protein folding and therefore the lack of a theoretical method to treat the problem. However, the newly proposed quantum folding theory affords a sound basis for discussing and studying these problems. In fact, photon emission or absorption in protein folding and the inelastic scattering of photons on proteins, as an electromagnetic process, can be accurately described by quantum electrodynamics. Because the electronic transition emitting or absorbing photon is coupled to the conformational change of a protein; the torsion transition in a polypeptide chain plays an important role in determining the photon emission/absorption rates or cross sections. We shall make the first-principle-calculation on the rates and cross sections of these photo-folding processes based on quantum electrodynamics. The quantitative results will provide several checkpoints on the quantum folding theory. The experimental tests of these theoretical predictions will provide refined evidence on the quantum nature of protein folding and photo-folding.

1 Theoretical method: deduction of protein photo-folding from quantum folding theory

1.1 Hamiltonian for protein folding and photo-folding

A protein is regarded as a conformation (torsion coordinate $\theta = \{\theta_j\}$ mainly)—electron system. Protein folding is described by the Hamiltonian $H_1\left(\theta, \frac{\partial}{\partial\theta}\right) + H_2(\theta, x, \nabla)$. In adiabatic approximation the wave function of the system can be expressed as

$$M(\theta, x) = \psi(\theta)\varphi(x, \theta), \tag{1}$$

and these two factors satisfy:

$$H_2(\theta, x, \nabla)\varphi_\alpha(x, \theta) = \varepsilon^a(\theta)\varphi_\alpha(x, \theta), \tag{2}$$

$$\left\{H_1\left(\theta, \frac{\partial}{\partial\theta}\right) + \varepsilon^\alpha(\theta)\right\}\psi_{kn\alpha}(\theta) = E_{kn\alpha}\psi_{kn\alpha}(\theta), \tag{3}$$

where α denotes the electronic state and (k, n) refer to the conformation- and vibration-states, respectively. The Hamiltonian $H_1\left(\theta, \frac{\partial}{\partial\theta}\right)$ includes the kinetic energy term $\sum\left(-\frac{\hbar^2}{2I_j}\frac{\partial^2}{\partial\theta_j^2}\right)$ (I_j is the inertial moment of the jth mode) and the torsion potential term. The torsion potential generally has several minima with respect to each θ_i and near each minimum the potential can be approximately expressed by a potential of a harmonic oscillator. Any small asymmetry in the potential has been shown to cause a strong localization of the wave functions [1]. The localized conformational state is labeled by the quantum number k. Since the adiabatic wave function is not a rigorous eigenstate of the Hamiltonian H_1+H_2, there exists a transition between the adiabatic states that result from the off–diagonal elements of H_1+H_2. The transition describes the non-radiative protein folding [1].

Since H_2 contains the electronic kinetic energy term, from gauge invariance of Hamiltonian H_1+H_2 we obtain the electromagnetic interaction:

$$H_{\mathrm{EM}} = H_1^{(\mathrm{EM})} + H_2^{(\mathrm{EM})}, \tag{4}$$

$$H_1^{(\mathrm{EM})} = -\frac{e}{mc}\sum_{k\lambda}\frac{\hbar}{\sqrt{2\omega_k V_0}}(c_{k\lambda} + c_{k\lambda}^+)\boldsymbol{\varepsilon}_{k\lambda}\cdot(-i\nabla), \tag{5}$$

$$H_2^{(\mathrm{EM})} = \frac{e^2}{4mc^2V_0}\sum_{k\lambda}\sum_{k'\lambda'}\frac{\boldsymbol{\varepsilon}_{k\lambda}\cdot\boldsymbol{\varepsilon}_{k'\lambda'}}{\sqrt{\omega_k\omega_{k'}}}(c_{k\lambda}c_{k'\lambda'}^+ + c_{k\lambda}^+c_{k'\lambda'} + c_{k\lambda}c_{k'\lambda'} + c_{k\lambda}^+c_{k'\lambda'}^+), \tag{6}$$

where m is the electron mass, $c_{k\lambda}$ and $c_{k\lambda}^+$ are annihilation and production operators, respectively, for a photon with the wave vector $\boldsymbol{k}$, frequency ω_k and polarization $\boldsymbol{\varepsilon}_{k\lambda}$, and V_0 denotes the normalization volume. From the perturbation $H_1^{(\mathrm{EM})}$ to second order and $H_2^{(\mathrm{EM})}$ to first order we calculate three types of protein photo-folding processes: (i) the stimulated single photon emission and absorption accompanying protein folding; (ii) the spontaneous photon emission in protein folding; and (iii) the photon-protein resonance Raman scattering. All calculations are carried out by the quantum electrodynamics method. To simplify the

notation, the calculations are made in units of $\hbar = c = 1$, and only in the final results the Planck constant $\hbar$ and the velocity of light c are written explicitly.

1.2 Stimulated photon emission and absorption in protein folding

We initially discuss single photon absorption. Set $|i\rangle = |kn\alpha, \nu_{k\lambda}\rangle$ where $|kn\alpha\rangle \sim M_{kn\alpha}(\theta, x) = \psi_{kn\alpha}(\theta)\varphi_\alpha(x, \theta)$ and $\nu_{k\lambda}$ the photon number of the wave vector $\boldsymbol{k}$ and polarization $\boldsymbol{\varepsilon}_{k\lambda}$. For the multi-torsion case, $\theta = (\theta_1, \theta_2, ..., \theta_N)$ and $\psi_{kn\alpha}(\theta)$ is the product of the functions of the single argument. Likewise, set $|f\rangle = |k'n'\alpha', \nu_{k\lambda} - 1\rangle$ where $|k'n'\alpha'\rangle \sim M_{k'n'\alpha'}(\theta, x) = \psi_{k'n'\alpha'}(\theta)\varphi_{\alpha'}(x, \theta)$. The above process is depicted by the reaction equation:

$$\nu_{k\lambda} \text{ photons + protein in } (kn\alpha) \rightarrow$$
$$(\nu_{k\lambda} - 1) \text{ photons + protein in } (k'n'\alpha').$$

By using eq. (5) we obtain

$$\begin{aligned}\langle f | H_1^{(\mathrm{EM})} | i\rangle &= -\frac{e}{m}\frac{\sqrt{\nu_{k\lambda}}}{\sqrt{2\omega_k V_0}} \boldsymbol{P}_{k'n'\alpha';kn\alpha} \cdot \boldsymbol{\varepsilon}_{k\lambda} \\ &= -\frac{e}{m}\sqrt{\frac{\nu_{k\lambda}}{2\omega_k V_0}} \boldsymbol{P}_{\alpha'\alpha} \cdot \boldsymbol{\varepsilon}_{k\lambda} \int \psi^+_{k'n'\alpha'}(\theta)\psi_{kn\alpha}(\theta)\mathrm{d}\theta,\end{aligned} \tag{7}$$

where

$$\begin{aligned}\boldsymbol{P}_{k'n'\alpha';kn\alpha} &= \int M^+_{k'n'\alpha'}(\theta, x)(-i\hbar\nabla)M_{kn\alpha}(\theta, x)\mathrm{d}\theta\mathrm{d}x \\ &= \int \psi^+_{k'n'\alpha'}(\theta)\psi_{kn\alpha}(\theta)\mathrm{d}\theta \int \varphi^+_{\alpha'}(x, \theta_0)(-i\hbar\nabla)\varphi_\alpha(x, \theta_0)\mathrm{d}x \\ &= \boldsymbol{P}_{\alpha'\alpha} \int \psi^+_{k'n'\alpha'}(\theta)\psi_{kn\alpha}(\theta)\mathrm{d}\theta\end{aligned} \tag{8}$$

$\boldsymbol{P}_{\alpha'\alpha}$ is the matrix element of the electron momentum. In the above deduction of eq. (8), the Condon approximation, namely, the matrix element $\int \varphi^+_{\alpha'}(x, \theta)(-i\hbar\nabla)\varphi_\alpha(x, \theta)\mathrm{d}x$, which does not depend on θ, has been used. The overlap integral $\int \psi^+_{k'n'\alpha'}(\theta)\psi_{kn\alpha}(\theta)\mathrm{d}\theta$ of the vibration wave function can be calculated under the harmonic approximation of the torsion potential [1]. Note that because $\alpha' \neq \alpha$, the wave function $\psi_{kn\alpha}(\theta)$ and $\psi_{k'n'\alpha'}(\theta)$ are not orthogonal to each other and the overlap integral always exists even for $k' = k$. After taking into consideration the thermal average over the initial vibration states and the summation over the final vibration states we obtain the absorption rate:

$$W_a = \frac{\pi e^2}{m^2 V_0}\frac{\nu_{k\lambda}}{\overline{\omega'}\omega_k}\left|\boldsymbol{P}_{\alpha'\alpha} \cdot \boldsymbol{\varepsilon}_{k\lambda}\right|^2 I_V, \tag{9}$$

$$I_V = \sum_n \left|\int \psi^+_{k'n'\alpha'}(\theta)\psi_{kn\alpha}(\theta)\mathrm{d}\theta\right|^2 B(n, T) = \sum_{\{p_j\}}\prod_j I_{Vj}, \tag{10}$$

$$I_{Vj} = \exp\{-Q_j(2\overline{n}_j + 1)\}\left(\frac{\overline{n}_j + 1}{\overline{n}_j}\right)^{p_j/2} J_{p_j}(2Q_j\sqrt{\overline{n}_j(\overline{n}_j + 1)}) \tag{11}$$

with

$$\overline{n}_j = (e^{\beta\hbar\omega_j} - 1)^{-1}\left(\beta = \frac{1}{k_B T}\right), \tag{12}$$

$$Q_j = I_j\omega_j(\delta\theta_j)^2 / 2\hbar, \tag{13}$$

$$p_j = \frac{\delta E_j}{\hbar\omega_j}. \tag{14}$$

$B(n,T)$ represents the Boltzmann factor for the thermal average, ω_j (ω'_j) is the frequency parameter of the jth torsion harmonic potential in the initial (final) state, δE_j is the energy gap between the initial and final states (the minimum of the jth initial potential minus that of the jth final) and $\delta\theta_j$ is the angular displacement of the torsion potential (the position difference between two minima of the jth torsion potential). p_j represents the net change in the vibration quantum number for the torsion oscillator mode j, which satisfies the constraint:

$$\sum_j p_j = p \tag{15}$$

in the last summation of eq. (10). I_V is the Thermo-Averaged Overlap Integral (TAOI). By use of the asymptotic formula for the Bessel function [12]:

$$e^{-z}J_p(z) = (2\pi z)^{-1/2}\exp(-p^2/2z) \quad \text{for } z >> 1 \tag{16}$$

I_{Vj} can be simplified. Finally we obtain

$$I_V = \frac{1}{\sqrt{2\pi}}\exp\left(\frac{\Delta G}{2k_B T}\right)\left(\sum Z_j\right)^{-\frac{1}{2}}\exp\left(-\frac{(\Delta G)^2}{2(\hbar\overline{\omega})^2\sum Z_j}\right) \tag{17}$$

with

$$Z_j = (\delta\theta_j^2)\frac{k_B T}{\hbar^2}I_j, \tag{18}$$

$$\Delta G = \Delta E + \sum_j k_B T \ln\frac{\omega_j}{\omega'_j}, \tag{19}$$

$$\Delta E = \sum_j \delta E_j. \tag{20}$$

$\overline{\omega}$ is the average of the initial torsion frequencies ω_j over the oscillator mode j. In eq. (17) the energy gap ΔE has been replaced by the free energy decrease ΔG to take the torsion

frequency difference $\omega_j \neq \omega_j'$ into account [1]. I_V is a function of ω_j (or its average $\bar{\omega}$), ω_j' (or its average $\bar{\omega}'$), $(\delta\theta_j)^2$ (or its average $(\delta\theta)^2$) and δE_j (or its sum ΔE). Note that the simplified expression (17) is obtained when z_j>>1. For photo-folding with a conformational change, $k' \neq k$, the condition is always fulfilled. The single photon absorption cross section is obtained readily from (9):

$$\sigma_a = \frac{e^2}{\hbar c}\frac{\pi}{\bar{\omega}'\omega_k}\frac{\left|\boldsymbol{P}_{\alpha'\alpha}\cdot\boldsymbol{\varepsilon}_{k\lambda}\right|^2}{m^2} I_V(\bar{\omega},\ \bar{\omega}',\ \delta\theta,\ \Delta E). \tag{21}$$

The corresponding absorption rate is denoted by W_a. By comparison with the non-radiative folding rate [1]:

$$k_f = \frac{2\pi}{\hbar^2\bar{\omega}'} I_E I_V(\bar{\omega}^{pf},\ \bar{\omega}'^{pf},\ \delta\theta^{pf},\ \Delta E^{pf}), \tag{22}$$

where I_V is defined by eq. (10) and has the same simplified expression as eq. (17), and the matrix element of the electronic wave function I_E is given by

$$I_E = \frac{\hbar^4}{4}\left(\sum_j \frac{a_j}{I_j}\right)^2 = \frac{\hbar^4 A}{4{I_0}^2},\ a_j = \left\langle l_j^2 \right\rangle,\ A = \left(\sum_j a_j\right)^2, \tag{23}$$

where I_0 is the average inertial moment and l_j represents the magnetic quantum number of the electronic wave function $\varphi_\alpha(x,\theta)$. We obtain the ratio of rates:

$$\frac{W_a}{k_f} = 2\frac{e^2/(\hbar c)}{\hbar^2 m^2 \omega_k}\frac{I_0^2}{A}\left|\boldsymbol{P}_{\alpha'\alpha}\cdot\boldsymbol{\varepsilon}_{k\lambda}\right|^2 \frac{I_V(\bar{\omega},\ \bar{\omega}',\ \delta\theta,\ \Delta E)}{I_V(\bar{\omega}^{pf},\ \bar{\omega}'^{pf},\ \delta\theta^{pf},\ \Delta E^{pf})} F, \tag{24}$$

where $F = \frac{c\nu_{k\lambda}}{V_0}$ is the incident photon flux in the photo-folding process. Setting

$$\omega_k \sim 2\pi\times 10^{15},\quad I_0 \sim 10^{-37},\quad \left(\frac{\mathrm{P}}{mc}\right)^2 \sim 10^{-5},$$
$$A \sim 10 - 10^4 \quad \text{(all in CGS units)}$$

and

$$I_V(\bar{\omega},\ \bar{\omega}',\ \delta\theta,\ \Delta E) = I_V(\bar{\omega}^{pf},\ \bar{\omega}'^{pf},\ \delta\theta^{pf},\ \Delta E^{pf})$$

leads to $\frac{W_a}{k_f} \approx (10^{-23} - 10^{-26})F$. Consequently, when the photon flux is large enough, $F > 10^{23}$ cm^{-2} s^{-1}, the single photon absorption rate is comparable with the protein folding rate.

The double- and multi-photon absorption rates or cross sections can be calculated by the same method with the second and the higher order perturbations. As a general rule, the absorption rates contain the TAOI factor, I_V.

For a single-photon stimulated emission

$\nu_{k\lambda}$ photons+protein in $(kn\alpha)$ →
$(\nu_{k\lambda}+1)$ photons + protein in $(k'n'\alpha')$.

Set $\left|i\right\rangle = \left|kn\alpha, \nu_{k\lambda}\right\rangle$ and $\left|f\right\rangle = \left|k'n'\alpha', \nu_{k\lambda}+1\right\rangle$. Through calculating the matrix element $\left\langle i\right|H_1^{(\mathrm{EM})}\left|f\right\rangle$ the single-photon stimulated emission cross section is deduced as

$$\sigma_e = \frac{\pi e^2}{\hbar c m^2 \bar{\omega}'\omega_k}\frac{(\nu_{k\lambda}+1)}{\nu_{k\lambda}}\left|\boldsymbol{P}_{\alpha'\alpha}\cdot\boldsymbol{\varepsilon}_{k\lambda}\right|^2 I_V \quad (\nu_{k\lambda} \geqslant 1). \tag{25}$$

The double- and multi-photon stimulated emission can be calculated in the same way through the second and the higher order perturbations. All results contain the TAOI factor I_V.

1.3 Spontaneous emission in protein folding and the spectrum structure of photo-folding

Following the same perturbation approach and setting the initial photon number $\nu_{k\lambda} = 0$ in the above deduction of the stimulated emission, one obtains the single-photon spontaneous emission rate. The rate of the quantum transition from a given initial state $\left|i\right\rangle = \left|kn\alpha\right\rangle$ to the definite final state of $\nu_{k\lambda}$ photons $\left|f\right\rangle = \left|k'n'\alpha', \nu_{k\lambda}\right\rangle$ is

$$W_{fi} = 2\pi\,\delta(E_{k'n'\alpha'} + \omega_k - E_{kn\alpha})\left|\left\langle f\right|H_1^{(\mathrm{EM})}\left|i\right\rangle\right|^2. \tag{26}$$

In the spontaneous emission case, the frequency of the emitted photon is not given a priori because no stimulating electromagnetic field of given frequency exists. Adopting a continuous representation of the electromagnetic field expansion and replacing the sum over the photon final states $\frac{\sum_k}{V_0}$ by $\frac{\int \mathrm{d}^3k}{(2\pi)^3}$ we obtain the emission rate or partial width:

$$\Gamma_e = \frac{e^2}{\hbar c}\frac{\omega_k}{2c^2m^2}\left|\boldsymbol{P}_{\alpha'\alpha}\cdot\boldsymbol{\varepsilon}_{k\lambda}\right|^2 I_V,\quad \left(\omega_k = \frac{E_{kn\alpha} - E_{k'n'\alpha'}}{\hbar}\right). \tag{27}$$

The numerical estimate gives

$\Gamma_e \sim 10^8 I_V$ as $\omega_k \sim 2\pi\times 10^{15}$, $\left(\frac{\mathrm{P}}{mc}\right)^2 \sim 10^{-5}$ (all in CGS units).

As $I_V = 1$, eq. (27) is in accordance with Einstein spontaneous emission formulas. We find the spectral linewidth has been largely reduced because of the overlap integral factor I_V. In fact, a spectral line of the electronic transition from state α to α' has been broadened to a band consisting of numerous single spectral lines. The spectral shape function is determined by the δ-function $\delta(E_{k'n'\alpha'} + \hbar\omega_k - E_{kn\alpha})$. For an electronic transition of given frequency $\frac{1}{\hbar}(\varepsilon^{\alpha'}(\theta_0) - \varepsilon^{\alpha}(\theta_0))$

there are a band of spectral lines characterized by the transition $\alpha \to \alpha'$ but with different ($(k'n')$) and (kn) satisfying $\hbar\omega_{\boldsymbol{k}} = E_{kn\alpha} - E_{k'n'\alpha'}$.

1.4 Photon-protein resonance Raman scattering

Consider the inelastic scattering:

$\nu_{\boldsymbol{k}\lambda}$ photons in $(\boldsymbol{k}\lambda) + \nu_{\boldsymbol{k}'\lambda'}$ photons in $(\boldsymbol{k}'\lambda')$ + protein in $(kn\alpha)$ →

$(\nu_{\boldsymbol{k}\lambda} - 1)$ photons in $(\boldsymbol{k}\lambda) + (\nu_{\boldsymbol{k}'\lambda'} + 1)$ photons in $(\boldsymbol{k}'\lambda')$ +protein in $(k'n'\alpha')$.

Set $|i\rangle = |kn\alpha,\ \nu_{\boldsymbol{k}\lambda},\ \nu_{\boldsymbol{k}'\lambda'}\rangle$ and $|f\rangle = |k'n'\alpha',\ \nu_{\boldsymbol{k}\lambda} - 1,\ \nu_{\boldsymbol{k}'\lambda'} + 1\rangle$. The scattering matrix element:

$$T_{fi} = \langle f | H_2^{(\mathrm{EM})} | i\rangle + \sum_m \frac{\langle f | H_1^{(\mathrm{EM})} | m\rangle \langle m | H_1^{(\mathrm{EM})} | i\rangle}{E_i - E_m + i0^+}. \quad (28)$$

The first term of (28) is

$$\begin{aligned}\langle f | H_2^{(\mathrm{EM})} | i\rangle &= \frac{e^2}{2mV_0} \frac{\boldsymbol{\varepsilon}_{\boldsymbol{k}\lambda} \cdot \boldsymbol{\varepsilon}_{\boldsymbol{k}'\lambda'}}{\sqrt{\omega_{\boldsymbol{k}}\omega_{\boldsymbol{k}'}}} \sqrt{\nu_{\boldsymbol{k}\lambda}(\nu_{\boldsymbol{k}'\lambda'} + 1)} \\ &\quad \int M^+_{k'n'\alpha'}(\theta, x) M_{kn\alpha}(\theta, x) \mathrm{d}\theta \mathrm{d}x \\ &= \delta_{\alpha'\alpha} \frac{e^2}{2mV_0} \frac{\boldsymbol{\varepsilon}_{\boldsymbol{k}\lambda} \cdot \boldsymbol{\varepsilon}_{\boldsymbol{k}'\lambda'}}{\sqrt{\omega_{\boldsymbol{k}}\omega_{\boldsymbol{k}'}}} \sqrt{\nu_{\boldsymbol{k}\lambda}(\nu_{\boldsymbol{k}'\lambda'} + 1)} \\ &\quad \int \psi^+_{k'n'\alpha'}(\theta) \psi_{kn\alpha}(\theta) \mathrm{d}\theta. \end{aligned} \quad (29)$$

Similarly, by using

$$\begin{aligned}|m\rangle &= |k_I n_I \alpha_I,\ \nu_{\boldsymbol{k}\lambda} - 1,\ \nu_{\boldsymbol{k}'\lambda'}\rangle \quad \text{or} \\ &= |k_I n_I \alpha_I,\ \nu_{\boldsymbol{k}\lambda},\ \nu_{\boldsymbol{k}'\lambda'} + 1\rangle,\end{aligned}$$

the second term of (28) is obtained:

$$\begin{aligned}&\sum_m \frac{\langle f | H_1^{(\mathrm{EM})} | m\rangle \langle m | H_1^{(\mathrm{EM})} | i\rangle}{E_i - E_m + i0^+} \\ &= \frac{e^2}{2m^2 V_0} \frac{\sqrt{\nu_{\boldsymbol{k}\lambda}(\nu_{\boldsymbol{k}'\lambda'} + 1)}}{\sqrt{\omega_{\boldsymbol{k}}\omega_{\boldsymbol{k}'}}} \\ &\quad \times \sum_{k_I n_I \alpha_I} \left\{ \frac{(\boldsymbol{P}_{k'n'\alpha';k_I n_I \alpha_I} \cdot \boldsymbol{\varepsilon}_{\boldsymbol{k}'\lambda'}) \cdot (\boldsymbol{P}_{k_I n_I \alpha_I;kn\alpha} \cdot \boldsymbol{\varepsilon}_{\boldsymbol{k}\lambda})}{E_{kn\alpha} - E_{k_I n_I \alpha_I} + \omega_{\boldsymbol{k}} + i0^+} \right. \\ &\quad \left. + \frac{(\boldsymbol{P}_{k'n'\alpha';k_I n_I \alpha_I} \cdot \boldsymbol{\varepsilon}_{\boldsymbol{k}\lambda}) \cdot (\boldsymbol{P}_{k_I n_I \alpha_I;kn\alpha} \cdot \boldsymbol{\varepsilon}_{\boldsymbol{k}'\lambda'})}{E_{kn\alpha} - E_{k_I n_I \alpha_I} - \omega_{\boldsymbol{k}'} + i0^+} \right\},\end{aligned} \quad (30)$$

where $\boldsymbol{P}_{k'n'\alpha';kn\alpha}$ can be simplified by eq. (8) under the Condon approximation. $E_{k_I n_I \alpha_I}$ depends on α_I more strongly than $k_I n_I$ and there are a set of resonant intermediate states with the same α_I but different $k_I n_I$. The energy of the resonant band $\{k_I n_I \alpha_{IC}\}$ for a given $\alpha_I = \alpha_{IC}$ is denoted by E_{IC}. Leaving only the resonant term in the summation, near resonance has the following:

$$\begin{aligned}&\sum_{k_I n_I \alpha_I} \frac{(\boldsymbol{P}_{k'n'\alpha';k_I n_I \alpha_I} \cdot \boldsymbol{\varepsilon}_{\boldsymbol{k}'\lambda'}) \cdot (\boldsymbol{P}_{k_I n_I \alpha_I;kn\alpha} \cdot \boldsymbol{\varepsilon}_{\boldsymbol{k}\lambda})}{E_{kn\alpha} - E_{k_I n_I \alpha_I} + \omega_{\boldsymbol{k}} + i0^+} \\ &= \int \psi^+_{k'n'\alpha'}(\theta) \psi_{kn\alpha}(\theta) \mathrm{d}\theta \frac{(\boldsymbol{P}_{\alpha'\alpha_I} \cdot \boldsymbol{\varepsilon}_{\boldsymbol{k}'\lambda'}) \cdot (\boldsymbol{P}_{\alpha_I\alpha} \cdot \boldsymbol{\varepsilon}_{\boldsymbol{k}\lambda})}{E_{kn\alpha} - E_{IC} + \omega_{\boldsymbol{k}} + i0^+}.\end{aligned} \quad (31)$$

Similarly,

$$\begin{aligned}&\sum_{k_I n_I \alpha_I} \frac{(\boldsymbol{P}_{k'n'\alpha';k_I n_I \alpha_I} \cdot \boldsymbol{\varepsilon}_{\boldsymbol{k}\lambda}) \cdot (\boldsymbol{P}_{k_I n_I \alpha_I;kn\alpha} \cdot \boldsymbol{\varepsilon}_{\boldsymbol{k}'\lambda'})}{E_{kn\alpha} - E_{k_I n_I \alpha_I} - \omega_{\boldsymbol{k}'} + i0^+} \\ &= \int \psi^+_{k'n'\alpha'}(\theta) \psi_{kn\alpha}(\theta) \mathrm{d}\theta \frac{(\boldsymbol{P}_{\alpha'\alpha_I} \cdot \boldsymbol{\varepsilon}_{\boldsymbol{k}\lambda}) \cdot (\boldsymbol{P}_{\alpha_I\alpha} \cdot \boldsymbol{\varepsilon}_{\boldsymbol{k}'\lambda'})}{E_{kn\alpha} - E_{IC} - \omega_{\boldsymbol{k}'} + i0^+}.\end{aligned} \quad (32)$$

Since $\psi_{kn\alpha}(\theta)$ is the solution of the eigenvalue eq. (3), we have the completeness of the wave functions:

$$\sum_{k_I n_I} \psi_{k_I n_I \alpha_{IC}}(\theta) \psi^+_{k_I n_I \alpha_{IC}}(\theta') = \delta(\theta - \theta'). \quad (33)$$

The completeness of eq. (33) has been used in the above deduction of eqs. (31) and (32). Summing up the contribution from $H_1^{(\mathrm{EM})}$ and $H_2^{(\mathrm{EM})}$, and inserting eqs. (29)–(32) into eq. (28) we obtain the cross section of the quantum transition from the initial state *i* to a definite final state *f*:

$$\sigma_{fi} = \frac{2\pi V_0}{\nu_{\boldsymbol{k}\lambda}} \delta(E_{k'n'\alpha'} + \omega_{\boldsymbol{k}'} - E_{kn\alpha} - \omega_{\boldsymbol{k}}) |T_{fi}|^2. \quad (34)$$

After taking the thermal average over the initial torsion vibration states and summation over the final torsion states and photon states in the direction $d\Omega$ (multiplied by a factor $\int \mathrm{d}\omega_{\boldsymbol{k}'} \frac{\omega_{\boldsymbol{k}'}^2 V_0}{(2\pi)^3}$) we obtain

$$\frac{\mathrm{d}\sigma}{\mathrm{d}\Omega} = \left(\frac{e^2}{4\pi mc^2} \right)^2 (\nu_{\boldsymbol{k}'\lambda'} + 1) \frac{\omega_{\boldsymbol{k}'}}{\omega_{\boldsymbol{k}}} I_R I_V, \quad (35)$$

where I_V is the TAOI given by eq. (10) or (17) and

$$I_R = \frac{\left| \frac{1}{m} (\boldsymbol{P}_{\alpha'\alpha_I} \cdot \boldsymbol{\varepsilon}_{\boldsymbol{k}'\lambda'}) \cdot (\boldsymbol{P}_{\alpha_I\alpha} \cdot \boldsymbol{\varepsilon}_{\boldsymbol{k}\lambda}) \right|^2}{(E_{kn\alpha} - E_{IC} + \hbar\omega_{\boldsymbol{k}})^2 + \frac{\Gamma_{IC}^2}{4}} \quad (36)$$

or

$$I_R = \frac{\left| \frac{1}{m} (\boldsymbol{P}_{\alpha'\alpha_I} \cdot \boldsymbol{\varepsilon}_{\boldsymbol{k}\lambda}) \cdot (\boldsymbol{P}_{\alpha_I\alpha} \cdot \boldsymbol{\varepsilon}_{\boldsymbol{k}'\lambda'}) \right|^2}{(E_{kn\alpha} - E_{IC} - \hbar\omega_{\boldsymbol{k}'})^2 + \frac{\Gamma_{IC}^2}{4}} \quad (37)$$

is the Raman tensor and Γ_{IC} is the resonance width of the α_{IC} band. Eq. (35) is in accordance with Kramers-Heisenberg

cross section formulas [13] as $I_V = 1$. The factor $\frac{e^2}{4\pi mc^2}$ in eq. (35) represents the electron classical radius. After being excited to a higher quantum state by absorbing photons, the orbital electron of a protein can relax to its ground state by emitting a fluorescence photon. The inelastic cross section eq. (35) can be used to explain the distribution and polarization of fluorescence photons. The occurrence of I_V in eq. (35) indicates that the inelastic cross section obeys the same law of temperature dependence as in protein folding.

2 Results and discussion: test on the protein quantum folding theory

2.1 Common factors of the thermo-averaged overlap integral of the torsion vibration wave function

We have studied protein-photon interactions and deduced the photon absorption/emission cross section and Raman scattering section in protein folding. All these sections (transition rates) have been compared with usual non-radiative folding rates (without the interaction of a photon). The general features of all photo-protein cross sections are the proportionality of the cross section to the TAOI of the torsion vibration wave function (eqs. (10), (11) and (17)). The factor has also occurred in non-radiative folding rate formulas [1]. It is the generalization of the overlap integral of the single mode harmonic oscillators, which has been described in previous work [14], to represent multi-modes and non-equal frequencies between initial and final states. Since both the initial $\psi_{kn\alpha}$ and final $\psi_{k'n'\alpha'}$ are approximated by the harmonic oscillator wave function, the overlap integral I_V is determined by two sets of harmonic frequencies $\{\omega_j\}$ and $\{\omega'_j\}$, and by the energy gap δE_j and angular shift $\delta\theta_j$ between two potentials of the jth torsion modes ($j = 1, \ldots, N$). Although the overlapping wave functions in non-radiative folding are $\psi_{kn\alpha}$ and $\psi_{k'n'\alpha}$ with equal quantum number α while in photo-folding are $\psi_{kn\alpha}$ and $\psi_{k'n'\alpha'}$ with $\alpha' \neq \alpha$, both overlap integrals I_V's are the same functions of torsion potential parameters ω_j, ω'_j, $\delta\theta_j$ and δE_j. The analytical form of I_V (eq. (17)) shows how the transition rate depends on the frequency ratio $\frac{\omega_j}{\omega'_j}$ of the jth torsion potential, the potential energy difference δE_j and the angular shift $\delta\theta_j$. The overlap integral is classified into two categories: $k = k'$ (without conformational change) and $k \neq k'$ (with conformational change). The protein folding belongs to the second category, whereas the protein photo-folding may occur in both categories, with and without conformational changes.

The common factor of the overlap integral I_V provides important information on protein folding and photo-folding. The detailed comparison of two kinds of folding processes can provide evidence on the quantum nature of the folding mechanism.

2.2 Temperature dependence of stimulated photon emission and absorption, and resonance Raman scattering

The stimulated photon absorption and emission cross sections are given by eqs. (21) and (25), respectively. For high incident photon flux the stimulated cross sections are large enough to observe. The cross section of the inelastic photon-protein resonance Raman scattering is given by eq. (35). All these protein photo-folding processes contain the same TAOI factor I_V in their cross sections, which also occurs in the non-radiative folding rate. Since the temperature dependencies of these folding rates and sections are determined by the factor I_V, it indicates that the folding rates should obey the same temperature dependence. As is well known, the non-Arrhenius behavior of the protein folding rate vs. temperature is a long-standing unsolved problem. Biologists are interested in understanding why protein folding depends on temperature in such an unusual way [15]. However, from quantum folding theory, Luo and Lu have deduced a general formula for the temperature dependence of the non-radiative transition rate k_f [3]:

$$\frac{\mathrm{d}\ln k_f}{\mathrm{d}\left(\frac{1}{T}\right)} = \frac{\mathrm{d}\ln I_V}{\mathrm{d}\left(\frac{1}{T}\right)} = S + \frac{1}{2}T + RT^2, \tag{38}$$

$$S = \frac{\Delta E}{2k_B}\left(1 - \frac{\Delta E}{\varepsilon}\right), \qquad R = \frac{k_B}{2\varepsilon}\lambda^2, \tag{39}$$

where

$$\varepsilon = \bar{\omega}^2(\delta\theta)^2 \sum I_j \cong NI_0\bar{\omega}^2(\delta\theta)^2 \tag{40}$$

is a scale variable of the torsion energy, I_0 represents the average torsion inertial moment of atomic groups in the polypeptide, N is the number of the collective torsion modes of the polypeptide chain, $\delta\theta = \sqrt{\langle(\delta\theta_j)^2\rangle_{\mathrm{av}}}$ is the average angular shift of the torsion potential, and

$$\lambda = \sum_j \ln\frac{\omega_j}{\omega'_j} \cong N\ln\frac{\bar{\omega}}{\bar{\omega}'} \tag{41}$$

describes the effect of the non-equal initial frequency to final. Eq. (39) shows that the temperature dependence is decided by three torsion potential parameters, namely the energy gap ΔE, the average angular shift $\delta\theta$ (or $\bar{\omega}\delta\theta$ in ε) and the initial-to-final frequency ratio $\frac{\bar{\omega}}{\bar{\omega}'}$. In the vicinity of the melting temperature, T_c, the temperature dependence of ΔE should be considered. Suppose $\Delta E(T) = \Delta E(T_c) +$

$m(T-T_c)$ is near T_c. One obtains the same temperature dependence in eq. (38); however, eq. (39) is replaced by

$$S=\frac{\eta\Delta E(T_c)}{2k_B}\left(1-\frac{\eta\Delta E(T_c)}{\varepsilon}\right),$$
$$R=\frac{1}{2\varepsilon k_B T_f^2}(\Delta G_f-\eta\Delta E(T_c))^2, \tag{42}$$

where $\eta=1-\frac{mT_c}{\Delta E(T_c)}$ describes the structural susceptibility of the torsion potential near the melting temperature and ΔG_f the equilibrium folding free energy decrease measured at temperature T_f. Note that in this case, the three torsion potential parameters are replaced by ΔG_f, ε and $\eta\Delta E(T_c)$. Having deduced eqs. (38), (39) and (42), Luo and Lu successfully interpreted the experimental temperature dependencies of all known protein folding rates.

(i) They proved that for 15 proteins whose experimental data were available the temperature dependencies of the folding rate are all in agreement with eq. (38).

(ii) By using S, R and the equilibrium free energy as input, the torsion potential parameters for each protein were fully determined in a consistent manner. The temperature dependence of the folding and the unfolding rates of a protein can be deduced in a unifying approach. It has been proved that the mutants may have very different temperature dependencies of the folding rates by virtue of the varying torsion potential parameter ΔE that arise because of the mutation [16].

Since the photo-folding and the usual non-radiative folding have the same I_V factor, we can make predictions that the temperature dependence of photo-folding obeys the same eqs. (38)–(42), deduced from non-radiative folding. Figures 1 and 2 give two examples. Figure 1 describes the temperature dependence of $\ln k_f$ versus $1/T$ for Trpcage (PDB code 1L2Y). Figure 2 shows the dependence $\ln k_f$–$1/T$ for the WW domain of Pin（PDB code 1PIN). In depicting two curves the torsion potential parameters are taken from the non-radiative folding and the experimental $\ln k_f$ in non-radiative folding at given temperatures are plotted for reference. By taking the difference of the torsion potential between the initial and final electronic states into account, the torsion potential parameters ΔE, $\delta\theta$ and $\frac{\bar{\omega}}{\bar{\omega}'}$ of photo-folding are different from those in non-radiative folding, and they are in principle dependent on the emitted or absorbed photon frequency. However, the electronic state has an influence upon the torsion potential, mainly through ΔE. From eq. (39) we know that the ΔE influences the slope term S of $\ln k_f$–$1/T$ relation. If the potential gap ΔE in photo-folding is greater (smaller) than that in non-radiative folding, then the Arhenius curve of photo-folding should be more (less) steep than Figure 1 for 1L2Y or should add a negative (positive) correction on the slope of the curve presented in Figure 2 for 1PIN.

Note that in the deduction of the temperature dependence, eq. (38), the "high temperature approximation", $Z_j=(\delta\theta_j^2)\frac{k_BT}{\hbar^2}I_j>>1$ has been assumed for the Bessel function simplification (see eq. (16)). It requires

$$\left|\delta\theta_j\right|>\frac{\hbar}{\sqrt{k_BTI_j}}. \tag{43}$$

For a typical torsion inertial moment I_j = 10^{-37} g cm^2

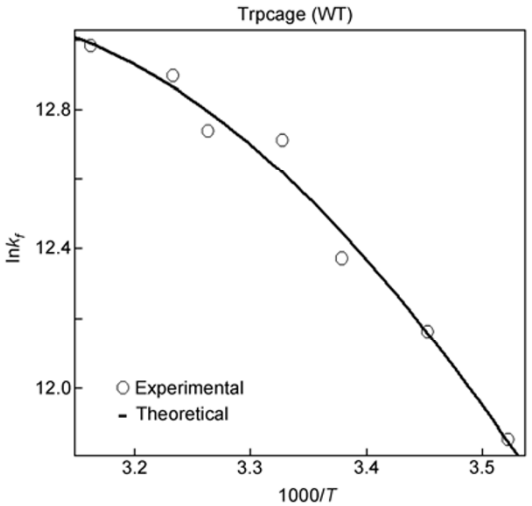

Figure 1 Arhenius plot for Tryptophan cage (1L2Y) folding. The parameters used in drawing the theoretical curve were taken as ΔG_f= −0.7 kcal mol^{-1} (T_f = 296), $\eta\Delta E(T_c)$=9.0k_BT_f, ε = 0.59k_BT_f, or $\delta\theta$ = 0.12; N = 18 [3]. The experimental $\ln k_f$ of the non-radiative folding at given temperatures can be found in [17].

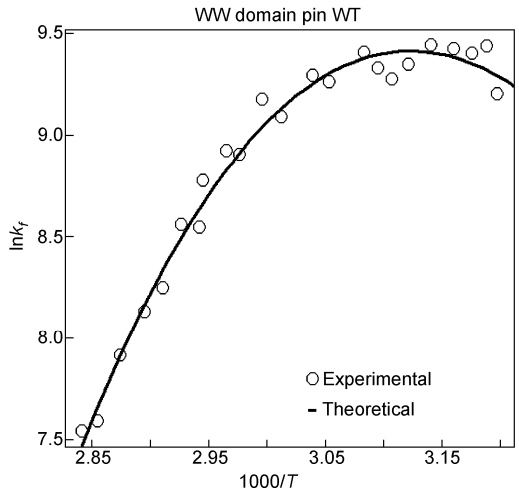

Figure 2 Arhenius plot for the WW domain of Pin (1PIN) folding. The parameters used in drawing the theoretical curve are taken as ΔG_f= −1.9 kcal mol^{-1} (T_f = 312), $\eta\Delta E(T_c)$ = 43.5k_BT_f, ε = 3.85k_BT_f, or $\delta\theta$ = 0.13; N = 99 [3]. The experimental $\ln k_f$ of the non-radiative folding at given temperatures can be found in [17].

it means that $\delta\theta_j > 1.6\times10^{-2}$, which can be fulfilled in the case of conformational change, $k \neq k'$. However, for photon emission and absorption accompanying small structural relaxation, the protein conformational change may not occur (i.e., $k' = k$) and the angular shift may be small. If eq. (43) is not fulfilled, then the original expressions (10) and (11) for the TAOI should be used instead of eq. (17), and the temperature dependence of the folding rate, eq. (38), should be modified.

2.3 Broadening of the spectral line and structure of the electronic spectrum in protein photo-folding

The motion of orbital electrons obeys the wave equation, eq. (2). In a given macromolecular configuration $\theta = \theta_0$, the energy is $\varepsilon^{\alpha}(\theta_0)$ and the emitted photon frequency is $\omega_k = \frac{1}{\hbar}(\varepsilon^{\alpha}(\theta_0) - \varepsilon^{\alpha'}(\theta_0))$ as the electron jumps from α to α'. However, because of the coupling between the structure of a protein and electron motion, the electronic jump inevitably causes protein structural relaxation or conformational changes. That is, the quantum state of the conformation-electron system changes from $M_{kn\alpha}(\theta, x)$ to $M_{k'n'\alpha}(\theta, x)$ because of the electronic transitions. The protein structure variation, in turn, makes the frequency of the emitted photon shift from ω_k to $\omega_k + \Delta\omega_k$ with

$$\Delta\omega_k = \frac{1}{\hbar}(E_{kn\alpha} - E_{k'n'\alpha'}) - \frac{1}{\hbar}(\varepsilon^{\alpha}(\theta_0) - \varepsilon^{\alpha'}(\theta_0)). \quad (44)$$

Thus the electronic transition spectrum is broadened and a spectral band is formed that corresponds to the electronic transition $\alpha \rightarrow \alpha'$. The band includes the abundant vibration spectrum without and with the conformational transition. The former corresponds to $k = k'$ and the latter corresponds to $k \neq k'$. The width of the spectral band is determined by the torsion vibration frequency. For example, for the spectral line $\omega_k \sim 2\pi\times10^{15}\ \mathrm{s}^{-1}$, the band width is in the order of $10^{13}\ \mathrm{s}^{-1}$, one hundredth or thousandth of the line frequency, and it consists of a large amount of transitions between α and α' in several tens of vibration energy levels.

Now we discuss the width of each spectral line in the band. The rate of spontaneous emission of a photon in protein folding is given by eq. (27). It contains the overlap integral factor I_V. The reason can be explained by the following argument. If an electron jumps from one orbital to another in the same molecular harmonic potential the transition will obey a strong selection rule and all transitions with changing vibration quantum number will be forbidden because of the orthogonality of the wave functions $\psi_{kn\alpha}(\theta)$ and $\psi_{kn'\alpha}(\theta)$ $(n \neq n')$. However, for an electronic transition with an initial and final torsion vibration in different harmonic potentials the vibration wave functions $\psi_{kn\alpha}(\theta)$ and $\psi_{k'n'\alpha'}(\theta)$ cannot be orthogonal to each other and the overlap integral exists. This is the so-called 'forbidden' transition. The overlap integral TAOI is an important determinant factor of the 'forbidden' transition rate. In the preceding calculation of a single-photon emission we estimate $\Gamma_e \sim 10^8 I_V\ \mathrm{s}^{-1}$. I_V changes over a wide range. From eqs. (17) and (18) the following is found:

$$\frac{\mathrm{d}\ln I_V}{\mathrm{d}(\delta\theta)^2} = -\frac{1}{2}\frac{1}{(\delta\theta)^2} + \frac{(\Delta G)^2}{2NI_0\bar{\omega}^2 k_B T}\frac{1}{(\delta\theta)^4}. \quad (45)$$

This equation gives rise to I_V taking a maximum at $(\delta\theta)^2_{\max} = \frac{(\Delta G)^2}{NI_0\bar{\omega}^2 k_B T}$. The typical value of $(I_V)_{\max}$ is 10^{-5}–10^{-4}. In the left of the maximum, $(\delta\theta)^2 < (\delta\theta)^2_{\max}$, I_V rapidly decreases as $\delta\theta \rightarrow 0$ following $\exp\left\{-\frac{\mathrm{const}}{(\delta\theta)^2}\right\}$. In the right of the maximum, I_V approximately changes with $(\delta\theta)^{-1}$. Assuming $I_V \sim 10^{-5}$ we obtain $\Gamma_e \sim 10^3\ \mathrm{s}^{-1}$. A typical lifetime for an atomic energy state is about 10^{-8} s, corresponding to a natural linewidth of about 6.6×10^{-8} eV. Therefore, the width Γ_e of the spectral line in protein photo-folding is five orders smaller than the natural linewidth. Moreover, due to its exponential dependence on $(\delta\theta)^2$, I_V may take a value much lower than 10^{-5} for small $\delta\theta$. This leads to the extra-narrowness of the width Γ_e. This is a well-marked characteristic of the photo-folding spectral lines.

2.4 Conclusion

Protein photo-folding—protein folding with photon absorption or emission and the inelastic scattering of a photon on a folded protein—is a useful field for experimentally determining whether protein folding obeys quantum laws. The particular form of the same temperature dependence (eq. (38)) for protein non-radiative folding and photo-folding, and the dominant structure of the photo-folding spectral band that consists of many narrow lines are two primary results deduced from protein quantum folding theory. These results are closely related to the fundamental aspects of quantum laws. First, the results imply the existence of a set of quantum oscillators in the transition process and these oscillators consist primarily of the torsion-vibration type of low frequency. Second, the results indicate that quantum tunneling does exist in protein folding, which means the non-locality of the state and the quantum coherence of conformational-electronic motion. The coherence is rooted deeply in the cooperative motion of many structural constituents (e.g., atomic electrons, molecular torsions) under a given temperature. Experimental tests on the above predictions are required and these studies will provide clearer ev-

idence on the quantum nature of protein folding and photo-folding.

The author is indebted to Drs. Lu Jun and Zhang Ying for numerous discussions on the experimental data analysis of the protein folding rates. This work was supported by the National Natural Science Foundation of China (Grant Nos. 202015 and 205015).

1 Luo L F. Protein folding as a quantum transition between conformational states. Front Phys, 2011, 6: 133–140
2 Zhang Y, Luo L F. The dynamical contact order: protein folding rate parameters based on quantum conformational transitions. Sci China Life Sci, 2011, 54: 386–392
3 Luo L F, Lu J. Temperature dependence of protein folding deduced from quantum transition. arXiv:1102.3748 [q-bio.BM], 2011. http://arxiv.org/abs/1102.3748
4 Frohlich H. Bose condensation of strongly exited longitudinal electric modes. Phys Lett, 1968, 26A: 402–403
5 Frohlich H. Collective behavior of non-linearly coupled oscillating fields. Collective Phenomenon, 1973, 1: 101–109
6 Shakhnovich E I. Theoretical studies of protein-folding thermodynamics and kinetics. Curr Opin Struct Biol, 1997, 7: 29–40
7 Baker D. A surprising simplicity to protein folding. Nature, 2000, 405: 39–42
8 Nishima W, Qi G, Hayward S, *et al*. DTA: dihedral transition analysis for characterization of the effects of large main-chain dihedral changes in proteins. Bioinformatics, 2009, 25: 628–635
9 Dill K A, Ozkan S B, Weiki T R, *et al*. The protein folding problem: when will it be solved? Curr Opin Struct Biol, 2007, 17: 342–346
10 Chalfie M. GFP: Lighting up life. Proc Natl Acad Sci USA, 2009, 106: 10073–10080
11 Neuweile H, Johnson C M, Fersht A R. Direct observation of ultrafast folding and denatures state dynamics in single protein molecules. Proc Natl Acad Sci USA, 2009, 106: 18569–18574
12 Watson G N. A Treatise on the Theory of Bessel Functions. 2nd ed. Series: Cambridge Mathematical Library, 1995
13 Louisell W. Quantum Statistical Properties of Radiation. New York: Wiley, 1973
14 Don Devault. Quantum mechanical tunneling in biological systems. Quart Rev Biophysics, 1980, 13**:** 387-564
15 Kentucky F C. Physicists discover quantum law of protein folding. 2011. http://www.technologyreview.com/blog/arxiv/26421/
16 Yang W Y, Gruebele M. Rate-temperature relationship in λ-repressor fragment $\lambda_{6\text{-}85}$ folding. Biochemistry, 2004, 43: 13018–13025
17 Kubelka J, Hofrichter J, Eaton W A. The protein folding speed limit. Curr Opin Struct Biol, 2004, 14: 76–88

Open Access This article is distributed under the terms of the Creative Commons Attribution License which permits any use, distribution, and reproduction in any medium, provided the original author(s) and source are credited.